

New Ternary Group-IV Tellurides with Extensive Te–Te Bonding: The Low-Dimensional Compounds $\text{Cs}_3\text{Ti}_3\text{Te}_{11}$ and $\text{Cs}_5\text{Hf}_5\text{Te}_{26}$

Michael A. Pell and James A. Ibers*

Department of Chemistry, Northwestern University, Evanston, Illinois 60208-3113

Received December 4, 1995. Revised Manuscript Received April 16, 1996[®]

The new compounds $\text{Cs}_3\text{Ti}_3\text{Te}_{11}$ and $\text{Cs}_5\text{Hf}_5\text{Te}_{26}$ have been synthesized from a Cs_2Te_n reactive flux. $\text{Cs}_3\text{Ti}_3\text{Te}_{11}$ crystallizes in the monoclinic space group $\text{C}_{2h}^5\text{-P}2_1/n$ with four formula units in a cell of dimensions $a = 10.776(4)$ Å, $b = 15.281(5)$ Å, $c = 14.843(5)$ Å, $\beta = 92.29(1)$ °, $V = 2442(2)$ Å³ ($T = 115$ K). The structure has been refined to an agreement index of $R_w(F^2)$ of 0.084 for 154 variables and 4812 observations; the value of R_I (on F for $F_o^2 > 2\sigma(F_o^2)$) is 0.034. $\text{Cs}_5\text{Hf}_5\text{Te}_{26}$ crystallizes in the monoclinic space group $\text{C}_{2h}^5\text{-P}2_1/c$ with four formula units in a cell of dimensions $a = 19.256(10)$ Å, $b = 9.487(6)$ Å, $c = 27.94(2)$ Å, $\beta = 98.40(8)$ °, $V = 5049(5)$ Å³ ($T = 115$ K). This structure has been refined to an agreement index of $R_w(F^2)$ of 0.171 for 145 variables and 3496 observations; the value of R_I (on F for $F_o^2 > 2\sigma(F_o^2)$) is 0.084. Both structures comprise chains of Te-bridged group-IV metals and both feature extensive Te–Te bonding within the chains. In $\text{Cs}_3\text{Ti}_3\text{Te}_{11}$ individual $[\text{Ti}_3\text{Te}_{11}^{3-}]$ chains are separated by Cs^+ cations to form a truly one-dimensional structure. The chains in $\text{Cs}_5\text{Hf}_5\text{Te}_{26}$ on the other hand are tethered through Te–Te interactions to form a pseudolayered structure. Assignment of oxidation states by an assessment of Te–Te bonding is not possible, owing to the plethora of intermediate Te–Te interactions. The electrical conductivity of $\text{Cs}_3\text{Ti}_3\text{Te}_{11}$ is $\approx 9.2 \times 10^{-5} \Omega^{-1} \text{ cm}^{-1}$ at 25 °C.

Introduction

The reactive-flux technique has proved to be especially fruitful in the synthesis of ternary alkali-metal group-IV chalcogenides (chalcogen = Q = S, Se, Te).^{1–4} These materials are characterized by a one-dimensional backbone of Te-bridged group-IV metals where each group-IV metal is coordinated to seven or more chalcogen anions. The individual metal–chalcogen chains are separated by alkali-metal cations. One fascinating aspect of these structures is that they typically contain a host of chalcogen–chalcogen interactions. In the sulfide and selenide compounds the bonding is unambiguous and S_2^{2-} and Se_2^{2-} units may be easily identified. Thus, $\text{K}_4\text{Ti}_3\text{S}_{14}$ ¹ and $\text{Na}_2\text{Ti}_2\text{Se}_8$ ² may be respectively formulated as $\text{K}_4[\text{Ti}_3(\text{S}_2)_6(\text{S})_2]$ and $\text{Na}_2[\text{Ti}_2(\text{Se}_2)_3(\text{Se})_2]$; these compounds contain Ti^{4+} . However, the related telluride compounds often possess distances intermediate to a Te–Te single bond (ca. 2.7 Å) and a van der Waals interaction (4.1 Å), and hence Te_n^{2-} ligands are often impossible to identify. This is illustrated effectively in the related compounds $\text{K}_4\text{M}_3\text{Te}_{17}$ ($\text{M} = \text{Zr, Hf}$)³ and $\text{Cs}_4\text{Zr}_3\text{Te}_{16}$.⁴ In $\text{K}_4\text{M}_3\text{Te}_{17}$ there are numerous Te–Te interactions in the range 2.76–4.10 Å. If the maximum Te–Te single bond length is arbitrarily taken to be 2.94 Å, the compound may be formulated as the M^{4+} compound $\text{K}_4[\text{M}_3(\text{Te}_3)(\text{Te}_2)_7]$. But in the related compound $\text{Cs}_4\text{Zr}_3\text{Te}_{16}$ such a facile, albeit arbitrary, assignment of oxidation states is not possible.

If, as in $\text{K}_4\text{M}_3\text{Te}_{17}$, the maximum Te–Te single bond length is taken to be 2.94 Å, the average oxidation state of Zr is +8.67. Obviously, an extension of the arbitrary Te–Te bonding limit is in order.

The materials presented here, namely, $\text{Cs}_3\text{Ti}_3\text{Te}_{11}$ and $\text{Cs}_5\text{Hf}_5\text{Te}_{26}$, are the newest members of the alkali-metal group-IV chalcogenide family and more specifically of the Cs/group IV/Te system. As for $\text{Cs}_4\text{Zr}_3\text{Te}_{16}$ they both possess numerous intermediate Te–Te interactions, and assignment of oxidation states is not possible.

Experimental Section

Syntheses of $\text{Cs}_3\text{Ti}_3\text{Te}_{11}$ and $\text{Cs}_5\text{Hf}_5\text{Te}_{26}$. Both compounds were synthesized from a low-melting Cs_2Te_3 reactive flux prepared from a stoichiometric addition of Te (Aldrich, 99.8%) to Cs (Aldrich, 99.5%) dissolved in liquid ammonia at –79 °C under an Ar atmosphere. The corresponding powders of the elements were then ground together, loaded into fused silica tubes, evacuated to 10^{-4} Torr, sealed, and placed in a tube furnace. The stoichiometries and heating profiles of the reactions are as follows: $\text{Cs}_3\text{Ti}_3\text{Te}_{11}$, Cs_2Te_3 was reacted with Ti (Johnson Matthey, 99.8%) and Te in a 2:3:10 ratio at 500 °C for 8 days and then cooled to 25 °C at 4 °C/h; $\text{Cs}_5\text{Hf}_5\text{Te}_{26}$, Cs_2Te_3 was reacted with Hf (Johnson Matthey, 99.6%) and Te in a 3:5:17 ratio at 900 °C for 6 days and then cooled to 25 °C at 4 °C/h. Both materials crystallize as black needles. Neither material could be obtained as a pure phase; invariably binary group-IV tellurides are present in the products. Needles of $\text{Cs}_5\text{Hf}_5\text{Te}_{26}$ are of minimum girth for X-ray diffraction examination and are of insufficient length for single-crystal four-probe electrical resistivity measurements; crystal size and quality preclude the collection of high-angle X-ray diffraction data (vide infra). Both compounds are stable in air and water. Semiquantitative energy-dispersive X-ray analysis (EDX) measurements confirmed the presence of the three elements in the respective compounds.

Crystallography. For both compounds preliminary lattice constants, Laue symmetry $2/m$, and space groups were de-

[®] Abstract published in *Advance ACS Abstracts*, June 1, 1996.

(1) Sunshine, S. A.; Kang, D.; Ibers, J. A. *J. Am. Chem. Soc.* **1987**, *109*, 6202–6204.

(2) Kang, D.; Ibers, J. A. *Inorg. Chem.* **1988**, *27*, 549–551.

(3) Keane, P. M.; Ibers, J. A. *Inorg. Chem.* **1991**, *30*, 1327–1329.

(4) Cody, J. A.; Ibers, J. A. *Inorg. Chem.* **1994**, *33*, 2713–2715.

Table 1. Crystal Data and Structure Refinement for $\text{Cs}_3\text{Ti}_3\text{Te}_{11}$ and $\text{Cs}_5\text{Hf}_5\text{Te}_{26}$

formula	$\text{Cs}_3\text{Ti}_3\text{Te}_{11}$	$\text{Cs}_5\text{Hf}_5\text{Te}_{26}$
fw	1946.03	4874.60
space group	$C_{2h}^5-P2_1/n$	$C_{2h}^5-P2_1/c$
a (Å) ^a	10.776(4)	19.256(10)
b (Å)	15.281(5)	9.487(6)
c (Å)	14.843(5)	27.94(2)
β , deg	92.29(1)	98.40(8)
V (Å ³)	2442(2)	5049(5)
ρ_{calcd} (g cm ⁻³)	5.293	6.413
Z	4	4
T (K) ^b	115	115
μ (cm ⁻¹)	182	285
transmission factors ^c	0.383–0.509	0.164–0.286
R (on F for $F_o^2 > 2\sigma(F_o^2)$)	0.034	0.084
$R_w(F^2)$	0.084	0.171

^a The cell parameters were obtained from a refinement constrained so that $\alpha = \gamma = 90^\circ$. ^b The low-temperature system is based on a design by Huffman.¹⁹ ^c The analytical method as employed in the Northwestern absorption program AGNOST was used for the absorption correction.

duced from Weissenberg photographs obtained at 25 °C. Final cell parameters were determined from the least-squares analysis of the setting angles of 33 reflections in the range $15^\circ < 2\theta(\text{Mo K}\alpha_1) < 35^\circ$ for $\text{Cs}_3\text{Ti}_3\text{Te}_{11}$ and 18 reflections in the range $33^\circ < 2\theta(\text{Mo K}\alpha_1) < 35^\circ$ for $\text{Cs}_5\text{Hf}_5\text{Te}_{26}$ automatically centered at 115 K on a Picker diffractometer. The intensities of six standard reflections measured every 100 reflections showed no significant change in intensity throughout data collection. Intensity data were processed⁵ and corrected for absorption⁶ by standard methods. Both structures were solved with the direct methods program XS in the SHELXTL program package⁷ and refined with the use of the program SHELXL-93.⁸ The final anisotropic refinement for $\text{Cs}_3\text{Ti}_3\text{Te}_{11}$ involved 154 variables and converged to agreement indexes $R_w(F^2)$ of 0.084 for all 4812 unique data and R_i of 0.034 for the 4141 data with $F_o^2 > 2\sigma(F_o^2)$. The final residual electron density map has no feature with a height greater than 4% that of a Ti atom. For $\text{Cs}_5\text{Hf}_5\text{Te}_{26}$ the final isotropic refinement involved 145 variables and converged to agreement indexes of $R_w(F^2)$ of 0.171 for all 3496 data and R_i of 0.084 for the 2088 data with $F_o^2 > 2\sigma(F_o^2)$. The final residual electron density map has no feature with a height greater than 6% that of a Te atom. Details of data collection and refinement are given in Tables 1 and S1.⁹ Positional parameters, equivalent isotropic displacement parameters for $\text{Cs}_3\text{Ti}_3\text{Te}_{11}$ and isotropic displacement parameters for $\text{Cs}_5\text{Hf}_5\text{Te}_{26}$ are given in Tables 2 and 3, respectively. Anisotropic displacement parameters for $\text{Cs}_3\text{Ti}_3\text{Te}_{11}$ can be found in Table S4.⁹

Electrical Conductivity of $\text{Cs}_3\text{Ti}_3\text{Te}_{11}$. Four gold wires with graphite extensions were attached with silver paint along the needle axis ([101]) of a 0.6 mm-long single crystal of $\text{Cs}_3\text{Ti}_3\text{Te}_{11}$. Two-probe dc measurements were made at 25 °C.

Results and Discussion

The structure of $\text{Cs}_3\text{Ti}_3\text{Te}_{11}$ comprises $[\text{Ti}_3\text{Te}_{11}]^{3-}$ chains separated by Cs^+ cations (Figure 1). Two of the Ti centers are coordinated to seven Te atoms in a pentagonal bipyramidal arrangement. The other Ti atom is coordinated in a distorted octahedral environment. The two pentagonal bipyramids share a common face, and each pair of pentagonal bipyramids is inter-

Table 2. Positional Parameters and Equivalent Isotropic Displacement Parameters for $\text{Cs}_3\text{Ti}_3\text{Te}_{11}$

atom	x	y	z	$U(\text{eq})$ (Å ²) ^a
Cs(1)	0.22400(6)	0.88088(4)	0.93786(4)	0.01827(14)
Cs(2)	0.08405(6)	1.03042(4)	0.65027(4)	0.01799(14)
Cs(3)	0.04875(6)	0.60858(4)	1.11988(4)	0.01602(14)
Ti(1)	0.02666(2)	0.70013(11)	0.67782(11)	0.0120(3)
Ti(2)	0.2754(2)	0.81053(11)	0.32096(11)	0.0118(3)
Ti(3)	0.1763(2)	0.78275(11)	0.51894(11)	0.0121(3)
Te(1)	0.23412(6)	0.93546(4)	0.45079(4)	0.01313(14)
Te(2)	0.24442(6)	0.78944(4)	0.69192(4)	0.01473(14)
Te(3)	0.40993(6)	0.69223(4)	1.05046(4)	0.01296(14)
Te(4)	-0.10922(6)	0.79729(4)	0.95537(4)	0.01341(14)
Te(5)	0.38044(6)	1.03545(4)	0.77971(4)	0.01472(14)
Te(6)	0.39883(6)	1.10758(4)	0.97947(4)	0.01332(14)
Te(7)	-0.12166(6)	0.84028(4)	0.73425(4)	0.01317(14)
Te(8)	0.10089(6)	0.84657(4)	1.18260(4)	0.01391(14)
Te(9)	0.33082(6)	0.93047(4)	1.18728(4)	0.01260(14)
Te(10)	0.03345(6)	0.66415(4)	0.86629(4)	0.01358(14)
Te(11)	0.55417(6)	0.78406(4)	0.86452(4)	0.01284(14)

^a $U(\text{eq})$ is defined as one-third of the trace of the orthogonalized U_{ij} tensor.

Table 3. Positional Parameters and Isotropic Displacement Parameters for $\text{Cs}_5\text{Hf}_5\text{Te}_{26}$

atom	x	y	z	$U(\text{Å}^2)$
Cs(1)	0.5393(3)	-0.2638(6)	0.9141(2)	0.026(2)
Cs(2)	0.1664(3)	-0.2659(6)	0.9121(2)	0.026(2)
Cs(3)	0.9113(3)	0.7376(6)	0.9163(2)	0.019(2)
Cs(4)	0.6943(4)	0.2151(8)	0.7241(3)	0.055(2)
Cs(5)	0.2923(3)	0.2176(6)	0.7225(2)	0.028(2)
Hf(1)	0.1281(2)	0.2032(4)	0.8810(2)	0.0136(11)
Hf(2)	0.3248(2)	0.1941(4)	0.87547(14)	0.0135(12)
Hf(3)	0.5255(2)	0.2041(4)	0.87496(14)	0.0119(11)
Hf(4)	0.7270(2)	0.2099(4)	0.87882(14)	0.0139(12)
Hf(5)	0.9289(2)	0.2094(4)	0.88337(14)	0.0153(12)
Te(1)	0.0417(3)	0.0720(6)	0.9458(2)	0.017(2)
Te(2)	0.0182(3)	-0.0043(6)	0.8442(2)	0.010(2)
Te(3)	0.0284(3)	0.4355(6)	0.8759(2)	0.012(2)
Te(4)	0.0099(4)	0.5142(7)	0.7732(2)	0.038(2)
Te(5)	0.1736(3)	0.3623(6)	0.9740(2)	0.016(2)
Te(6)	0.1151(3)	0.2580(6)	0.7755(2)	0.014(2)
Te(7)	0.2458(3)	0.1259(6)	0.9537(2)	0.009(2)
Te(8)	0.2095(3)	0.0347(6)	0.8189(2)	0.011(2)
Te(9)	0.2194(3)	0.4106(6)	0.8409(2)	0.008(2)
Te(10)	0.3501(3)	-0.1075(6)	0.9000(2)	0.016(2)
Te(11)	0.3432(3)	0.4691(6)	0.9224(2)	0.016(2)
Te(12)	0.4444(3)	0.1156(6)	0.9495(2)	0.011(2)
Te(13)	0.4173(3)	0.0217(6)	0.8212(2)	0.013(2)
Te(14)	0.4159(3)	0.4170(6)	0.8443(2)	0.008(2)
Te(15)	0.5434(3)	0.3562(6)	0.9672(2)	0.013(2)
Te(16)	0.5024(3)	0.2176(6)	0.7679(2)	0.016(2)
Te(17)	0.6378(3)	0.1319(6)	0.9529(2)	0.013(2)
Te(18)	0.6170(3)	0.0270(6)	0.8248(2)	0.010(2)
Te(19)	0.6211(3)	0.4212(6)	0.8435(2)	0.011(2)
Te(20)	0.7190(3)	-0.0939(6)	0.9015(2)	0.016(2)
Te(21)	0.7205(3)	0.4905(6)	0.9233(2)	0.016(2)
Te(22)	0.8411(3)	0.1393(6)	0.9564(2)	0.010(2)
Te(23)	0.8184(3)	0.0459(6)	0.8223(2)	0.014(2)
Te(24)	0.8205(3)	0.4227(6)	0.8441(2)	0.012(2)
Te(25)	0.9305(3)	0.3665(6)	0.9775(2)	0.014(2)
Te(26)	0.8939(3)	0.2636(6)	0.7787(2)	0.011(2)

connected through face sharing with an octahedron (Figure 2). To achieve this connectivity, the chain must buckle, as there are no parallel faces in a pentagonal bipyramidal. A similar buckling occurs in the $\text{Na}_2\text{Ti}_2\text{Se}_8$ structure in which Ti cations are also seven coordinate. This is not unexpected as Ti, the smallest group-IV metal, will be able to accommodate the smaller coordination sphere necessary for face sharing. Although technically the $\text{K}_4\text{M}_3\text{Te}_{17}$ ($\text{M} = \text{Zr}, \text{Hf}$) and $\text{Cs}_4\text{Zr}_3\text{Te}_{16}$ structures are based on a face-sharing framework, it is a trigonal prismatic framework in which metal–telurium distances are extended. Selected bond distances

(5) Waters, J. M.; Ibers, J. A. *Inorg. Chem.* **1977**, *16*, 3273–3277.

(6) de Meulenaer, J.; Tompa, H. *Acta Crystallogr.* **1965**, *19*, 1014–1018.

(7) Sheldrick, G. M. SHELXTL PC Version 5.0 An Integrated System for Solving, Refining, and Displaying Crystal Structures from Diffraction Data; Siemens Analytical X-Ray Instruments, Inc.: Madison, WI, 1994.

(8) Sheldrick, G. M. *J. Appl. Crystallogr.* **1996**; in preparation.

(9) Supporting information (see paragraph at end of paper).

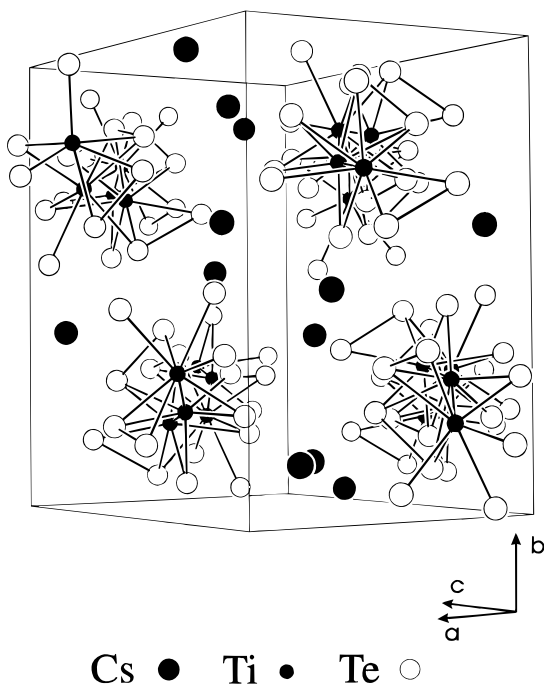


Figure 1. Unit cell of $\text{Cs}_3\text{Ti}_3\text{Te}_{11}$. Te–Te bonds are shown for interactions less than 2.9 Å. Here and in subsequent figures atoms are drawn as circles of arbitrary size.

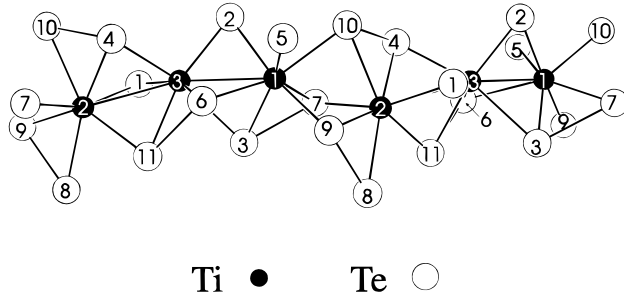


Figure 2. ${}^1[\text{Ti}_3\text{Te}_{11}^{3-}]$ chain. Te–Te bonds are shown for interactions less than 2.9 Å.

Table 4. Selected Bond Lengths (Å) for $\text{Cs}_3\text{Ti}_3\text{Te}_{11}^a$

Ti(1)–Te(2)	2.716(2)	Ti(3)–Te(1)	2.628(2)
Ti(1)–Te(3) (#1)	2.769(2)	Ti(3)–Te(2)	2.644(2)
Ti(1)–Te(5) (#2)	2.772(2)	Ti(3)–Te(11) (#1)	2.791(2)
Ti(1)–Te(7)	2.819(2)	Ti(3)–Te(6) (#2)	2.797(2)
Ti(1)–Te(10)	2.849(2)	Ti(3)–Te(4) (#4)	2.811(2)
Ti(1)–Te(6) (#2)	2.872(2)	Ti(3)–Te(3) (#1)	2.952(2)
Ti(1)–Te(9) (#1)	2.911(2)	Te(3)–Te(7) (#5)	2.807(1)
Ti(2)–Te(1)	2.761(2)	Te(4)–Te(10)	2.901(1)
Ti(2)–Te(9) (#3)	2.783(2)	Te(5)–Te(10) (#6)	3.096(1)
Ti(2)–Te(8) (#3)	2.784(2)	Te(5)–Te(6)	3.162(1)
Ti(2)–Te(4) (#4)	2.836(2)	Te(5)–Te(9) (#7)	3.173(2)
Ti(2)–Te(10) (#4)	2.861(2)	Te(6)–Te(11) (#7)	2.875(1)
Ti(2)–Te(7) (#4)	2.883(2)	Te(8)–Te(9)	2.788(1)
Ti(2)–Te(11) (#1)	2.884(2)		

^a Symmetry transformations used to generate equivalent atoms: #1, $x - \frac{1}{2}, -y + \frac{3}{2}, z - \frac{1}{2}$; #2, $-x + \frac{1}{2}, y - \frac{1}{2}, -z + \frac{3}{2}$; #3, $x, y, z - 1$; #4, $x + \frac{1}{2}, -y + \frac{3}{2}, z - \frac{1}{2}$; #5, $x + \frac{1}{2}, -y + \frac{3}{2}, z + \frac{1}{2}$; #6, $-x + \frac{1}{2}, y + \frac{1}{2}, -z + \frac{3}{2}$; #7 $-x + 1, -y + 2, -z + 2$.

for $\text{Cs}_3\text{Ti}_3\text{Te}_{11}$ are given in Table 4; Table S2⁹ presents further metrical details. The Ti–Te bond distances range from 2.628(2) to 2.952(2) Å and are comparable with those of 2.787(1) to 2.788(1) Å found in the structure of the compound CsTiUTe_5 .¹⁰ The Cs^+ cations exhibit coordination numbers 9, 10, and 12. Cs–Te

(10) Cody, J. A.; Ibers, J. A. *Inorg. Chem.* **1995**, *34*, 3165–3172.

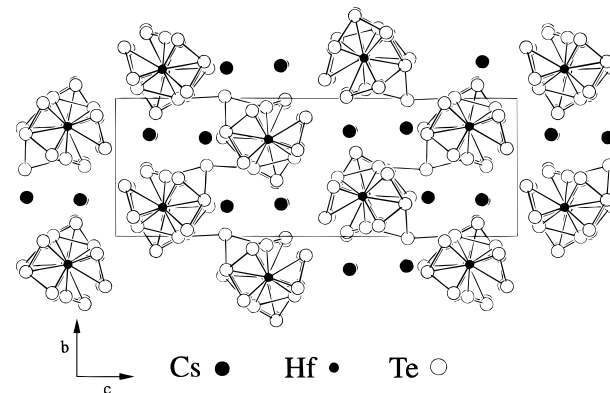


Figure 3. Unit cell of $\text{Cs}_5\text{Hf}_5\text{Te}_{26}$. Te–Te bonds are shown for interactions less than 3.3 Å.

distances span 3.662(1)–4.267(2) Å and agree with those found in the $\text{Cs}_4\text{Zr}_3\text{Te}_{16}$ structure (3.629(1)–4.456(1) Å).

There are three Te–Te interactions with distances less than 2.9 Å and four in the range 2.901(1)–3.173(2) Å in the structure of $\text{Cs}_3\text{Ti}_3\text{Te}_{11}$. If 2.901 Å is taken to be the maximum bonding distance, then the anionic chain takes the formula ${}^1[\text{Ti}_3(\text{Te}_2)_4(\text{Te})_3^{3-}]$; choosing 3.1 Å as the maximum bonding distance results in the formula ${}^1[\text{Ti}_3(\text{Te}_3)(\text{Te}_2)_3(\text{Te})_2^{3-}]$. To retain charge neutrality, the former anion must contain two Ti^{4+} and one Ti^{3+} center while the latter anion must contain three Ti^{3+} centers. While Ti^{3+} species have been previously observed in solid-state chalcogenides,^{11–14} there is no concrete evidence that such an oxidation state exists here; insufficient material precludes the measurement of the magnetic susceptibility of $\text{Cs}_3\text{Ti}_3\text{Te}_{11}$. At 25 °C the conductivity of $\text{Cs}_3\text{Ti}_3\text{Te}_{11}$ is $\approx 9.2 \times 10^{-5} \Omega^{-1} \text{ cm}^{-1}$; at 77 K the conductivity is too low to be measured on our apparatus. The material is a semiconductor. Ti–Ti separations along the ${}^1[\text{Ti}_3\text{Te}_{11}^{3-}]$ chain are 3.172(2) (Ti(1)–Ti(3)) and 3.195(3) Å (Ti(2)–Ti(3)). The Ti–Ti separation of 2.97 Å in elemental Ti (A3-type)¹⁵ suggests that there might be some Ti–Ti bonding in the form of Ti(1)–Ti(3)–Ti(2) trimers in the structure of $\text{Cs}_3\text{Ti}_3\text{Te}_{11}$. Perhaps the semiconducting nature in spite of the postulated $\text{Ti} \text{d}^1$ configuration arises from the localization of the d^1 electrons in Ti–Ti bonds.

As in the related $\text{K}_4\text{M}_3\text{Te}_{17}$ ($\text{M} = \text{Zr, Hf}$) and $\text{Cs}_4\text{Zr}_3\text{Te}_{16}$ structures, the structure of $\text{Cs}_5\text{Hf}_5\text{Te}_{26}$ (Figure 3) is based on a framework of group-IV metal atoms coordinated to Te ligands in a bicapped trigonal prismatic fashion (Figure 4). These polyhedra share triangular faces along the [010] direction. Whether this material is truly one-dimensional or is actually a layered structure (as it is drawn in the figures) will be addressed below. Hf–Te and Te–Te distances are provided in Table 5; more metrical details may be found in Table S3.⁹ The Hf–Te bond distances range from 2.891(7) to 3.020(7) Å and are consistent with those found in the $\text{Cs}_4\text{Hf}_3\text{Te}_{16}$ structure (2.878(1)–3.087(1) Å). Three of the unique Cs^+ cations are coordinated to 11 Te anions

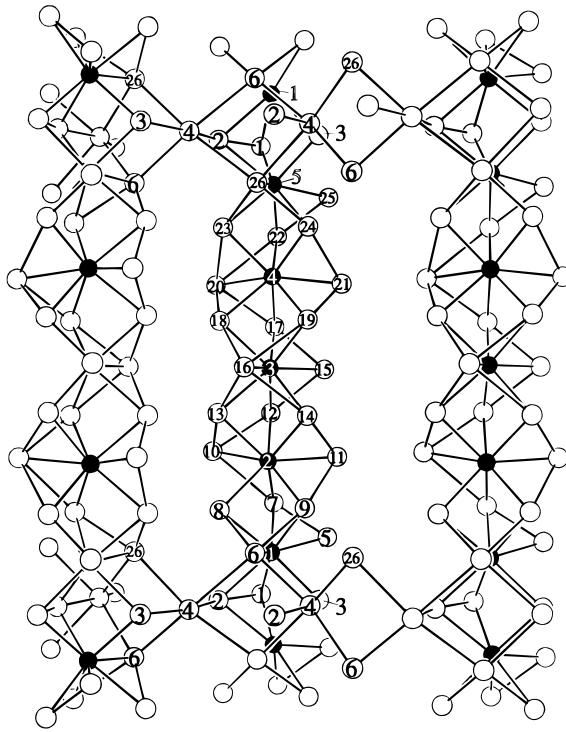
(11) Mähl, D.; Pickardt, J.; Reuter, B. *Z. Anorg. Allg. Chem.* **1982**, *491*, 203–207.

(12) Quint, R.; Boller, H. *Mater. Res. Bull.* **1987**, *22*, 1499–1504.

(13) Haange, R. J.; Bos-Alberink, A. J. A.; Wiegers, G. A. *Ann. Chim. (Paris)* **1978**, *3*, 201–207.

(14) Saidi, Y.; Abrahams, I.; Bruce, P. G. *Mater. Res. Bull.* **1990**, *25*, 533–538.

(15) Hull, A. W. *Phys. Rev.* **1921**, *18*, 88–89.



Hf • Te ○

Figure 4. Pseudolayer of $[\text{Hf}_5\text{Te}_{26}^{5-}]$. The Te–Te bond range has been extended to 3.5 Å to show the octahedral environment and connectivity of the Te(4) atom.

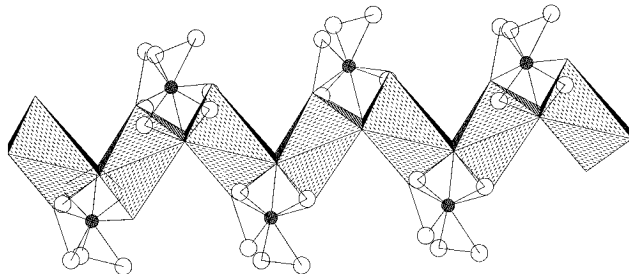


Figure 5. Edge-sharing TeTe_6 octahedra running along [010] sew together the Hf chains.

whereas the other two are coordinated to 12 Te anions. The Cs–Te interactions (3.726(10)–4.386(8) Å) are in agreement with those in the $\text{Cs}_4\text{Zr}_3\text{Te}_{16}$ and $\text{Cs}_3\text{Ti}_3\text{Te}_{11}$ structures. There are 15 Te–Te separations less than 3 Å, eight between 3.0 and 3.3 Å, and seven between 3.3 and 3.6 Å. The assignment of oxidation states in $\text{Cs}_5\text{Hf}_5\text{Te}_{26}$ is not possible.

There is one peculiar feature to this structure. Atom Te(4) has no significant interactions with Hf or Cs centers. It resides in a distorted octahedral environment, surrounded by six other Te anions, in which Te–Te distances range from 2.935(9) to 3.470(9) Å. Its anisotropic displacement parameters are considerably higher than those of the other Te atoms, consistent with it being only loosely bound to the structural framework. That the Te(4) site is fully occupied by Te and not by a lighter element was established from a refinement of its site occupancy which converged to a value of 1.00-(2). Moreover, no other elements were detected in EDX measurements on the crystal used for data collection. The existence of a TeTe_6 octahedron is not unprecedented. The structure of elemental Te (A8-type)

Table 5. Selected Bond Lengths (Å) for $\text{Cs}_5\text{Hf}_5\text{Te}_{26}^a$

Hf(1)–Te(7)	2.907(7)	Hf(5)–Te(26)	2.947(7)
Hf(1)–Te(3)	2.913(7)	Hf(5)–Te(23)	2.963(7)
Hf(1)–Te(1)	2.912(8)	Hf(5)–Te(2) (#4)	2.970(7)
Hf(1)–Te(2)	2.963(7)	Hf(5)–Te(24)	2.996(7)
Hf(1)–Te(6)	2.968(7)	Hf(5)–Te(25)	3.018(7)
Hf(1)–Te(9)	2.965(7)	Te(1)–Te(2)	2.901(9)
Hf(1)–Te(8)	2.969(7)	Te(2)–Te(4) (#1)	3.250(9)
Hf(1)–Te(5)	3.020(7)	Te(3)–Te(4)	2.935(9)
Hf(2)–Te(7)	2.912(7)	Te(4)–Te(6)	3.159(9)
Hf(2)–Te(11)	2.918(7)	Te(4)–Te(26) (#3)	3.281(9)
Hf(2)–Te(8)	2.947(7)	Te(4)–Te(26) (#4)	3.453(9)
Hf(2)–Te(9)	2.950(7)	Te(4)–Te(6) (#2)	3.470(9)
Hf(2)–Te(12)	2.957(7)	Te(5)–Te(7)	2.741(8)
Hf(2)–Te(14)	2.958(7)	Te(6)–Te(9)	2.898(8)
Hf(2)–Te(10)	2.967(7)	Te(6)–Te(8)	2.936(8)
Hf(2)–Te(13)	2.989(7)	Te(7)–Te(10)	3.474(9)
Hf(3)–Te(12)	2.903(7)	Te(9)–Te(11)	3.096(8)
Hf(3)–Te(17)	2.919(7)	Te(10)–Te(13)	2.977(9)
Hf(3)–Te(15)	2.930(7)	Te(10)–Te(12)	2.993(8)
Hf(3)–Te(18)	2.935(7)	Te(11)–Te(14)	2.803(9)
Hf(3)–Te(13)	2.946(7)	Te(12)–Te(15)	2.969(8)
Hf(3)–Te(14)	2.955(7)	Te(13)–Te(16)	3.012(9)
Hf(3)–Te(16)	2.961(7)	Te(14)–Te(16)	3.457(8)
Hf(3)–Te(19)	2.981(7)	Te(15)–Te(17)	2.864(9)
Hf(4)–Te(19)	2.926(7)	Te(16)–Te(18)	3.105(8)
Hf(4)–Te(22)	2.929(7)	Te(16)–Te(19)	3.464(8)
Hf(4)–Te(21)	2.948(7)	Te(17)–Te(20)	3.122(8)
Hf(4)–Te(20)	2.960(7)	Te(18)–Te(20)	2.922(9)
Hf(4)–Te(24)	2.961(7)	Te(19)–Te(21)	2.796(9)
Hf(4)–Te(23)	2.971(7)	Te(20)–Te(23)	3.400(9)
Hf(4)–Te(17)	2.970(8)	Te(20)–Te(22)	3.423(8)
Hf(4)–Te(18)	2.974(7)	Te(21)–Te(24)	3.202(9)
Hf(5)–Te(1) (#4)	2.891(7)	Te(22)–Te(25)	2.769(8)
Hf(5)–Te(3) (#4)	2.904(7)	Te(23)–Te(26)	2.894(8)
Hf(5)–Te(22)	2.910(8)	Te(24)–Te(26)	2.893(8)

^a Symmetry transformations used to generate equivalent atoms: #1, $-x, y - 1/2, -z + 3/2$; #2 $-x, y + 1/2, -z + 3/2$; #3, $x - 1, y, z$; #4, $-x + 1, y + 1/2, -z + 3/2$.

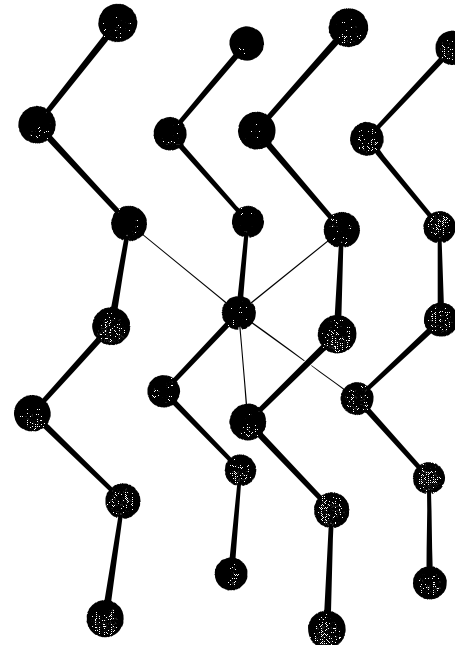


Figure 6. Octahedral coordination of Te in the crystal structure of elemental Te.

comprises helical Te_n chains in which the Te–Te bond distance is 2.8345(8) Å and the Te–Te–Te bond angle is 103.14(2)° (Figure 6).¹⁶ In addition to its two intra-chain Te neighbors, each Te center in metallic Te has

(16) Adenis, C.; Langer, V.; Lindqvist, O. *Acta Crystallogr., Sect. C: Cryst. Struct. Commun.* **1985**, *45*, 941–942.

four longer interchain contacts of 3.4912(8) Å. The resulting environment of each Te atom is octahedral with Te–Te–Te bond angles ranging from 79 to 89°. To our knowledge $\text{Cs}_5\text{Hf}_5\text{Te}_{26}$ represents the first example of the stabilization of such a Te coordination outside of the elemental Te structure.

Selected Te–Te distances are given in Table 5. If 3.00 Å is considered the maximum Te–Te bonding distance, then atoms Te(4) and Te(3) form a $\mu_2\text{-}\eta^1\text{-Te}_2^{2-}$ ligand. However, if this maximum is extended to 3.25 Å (a reasonable distance compared with the 3.492(6) Å Te–Te interaction in TiGeTe_6 ¹⁷ and the 3.506 Å Te–Te interaction in CrTe_3 ,¹⁸ which were both shown to have some bonding character), the Te(4) atom attaches to a Te(2) atom in an adjoining chain and links the two chains together. Figure 5 shows how the Te(4) octahe-

dra share edges along [010] in an undulating manner, forming a backbone onto which the chains are anchored. Whether or not the individual chains are joined together through bonds to form a layered structure we cannot answer unequivocally. There is certainly an interaction between individual chains, and we elect to describe this structure as two-dimensional or pseudolayered.

Acknowledgment. This work was supported by NSF Grant DMR 91-14934. This work made use of MRL Central Facilities supported by the National Science Foundation at the Materials Research Center of Northwestern University under Grant DMR 91-20521.

Supporting Information Available: Additional crystallographic details (Table S1), further metrical details (Tables S2 and S3), (27 pages); anisotropic displacement parameters (Tables S4) (38 pages). Ordering information is given on any current masthead page.

CM9505761

(17) Mar, A.; Ibers, J. A. *J. Am. Chem. Soc.* **1993**, *115*, 3227–3238.
(18) Canadell, E.; Jobic, S.; Brec, R.; Rouxel, J. *J. Solid State Chem.* **1992**, *98*, 59–70.
(19) Huffman, J. C. Ph.D. Dissertation, Indiana University, 1974.